



**Mineralogical and Chemical Composition of Saprolite from South Fork Brokenback Run
Watershed, Shenandoah National Park, Virginia**

Open-File Report 2006-1366

**U.S. Department of the Interior
U.S. Geological Survey**

U.S. Department of the Interior

Dirk Kempthorne, Secretary

U.S. Geological Survey

Mark D. Myers, Director

U.S. Geological Survey, Reston, Virginia 2006

For product and ordering information:

World Wide Web: <http://www.usgs.gov/pubprod>

Telephone: 1-888-ASK-USGS

For more information on the USGS—the Federal source for science
about the Earth,

its natural and living resources, natural hazards, and the environment:

World Wide Web: <http://www.usgs.gov>

Telephone: 1-888-ASK-USGS

The use of trade, product, or firm names is for identification purposes
only and does not imply endorsement by the U.S. Government.

Although this report is in the public domain, permission must be secured
from the individual copyright owners to reproduce any copyrighted
material contained within this report.

Contents

ABSTRACT	1
INTRODUCTION	1
METHODS	3
Saprolite Sampling	
Mineral Separation Technique	4
X-ray Diffraction Procedures	
Chemical Analysis	5
Estimating Mineral Abundance	6
Use of CLAYFORM to develop a clay-mineral formula	
MINERALOGICAL AND CHEMICAL COMPOSITION OF SAPROLITE	7
Mineralogy	
Chemical Analysis	8
CLAYFORM Results	
SUMMARY	10
ACKNOWLEDGMENTS	11
REFERENCES	11

Figures

1. Site map of South Fork Brokenback Run, Shenandoah National Park	12
--	----

Tables

	<u>page</u>
1. Description of Saprolite Weathering Profile at Old Rag Mountain (Core 2, OR83-2)	13
2. Description of Saprolite Weathering Profile at Old Rag Mountain (Core 3, OR83-3)	13
3. Mineral identification results of XRD analyses of bulk fraction ($> 1 \mu\text{m}$)	14
4a. Mineral identification results of XRD analyses of clay fraction ($< 1 \mu\text{m}$)	14
4b. Mineral identification results of XRD analyses of fine fraction ($< 0.5 \mu\text{m}$)	15
5a. Mineral identification results of XRD analyses of ultra-fine fraction ($< 0.1 \mu\text{m}$)	15
5b. Mineral identification results of XRD analyses of ultra-fine fraction ($< 0.03 \mu\text{m}$)	16
6. Chemical composition of bulk fraction ($> 1 \mu\text{m}$)	16
7. Chemical composition of fine fraction ($< 0.5 \mu\text{m}$)	17
8. Chemical composition of ultra-fine fraction ($< 0.1 \mu\text{m}$)	17
9. Chemical composition of ultra-fine fraction ($< 0.03 \mu\text{m}$)	17
10. Mineral formulae for interlayered smectite ($< 0.5 \mu\text{m}$ fraction)	18
11. Mineral formulae for interlayered smectite ($< 0.1 \mu\text{m}$ fraction)	19
12. Mineral formulae for interlayered smectite ($< 0.03 \mu\text{m}$ fraction)	19

Conversion Factors and Abbreviations

Multiply	By	To obtain
Length		
micrometer (μm)	0.0003937	inch (in.)
millimeter (mm)	0.03937	inch (in.)
meter (m)	3.281	foot (ft.)
kilometer (km)	0.6214	mile (mi.)
Area		
hectare	0.4047	Acre
square kilometer (km^2)	0.3861	square mile (mi^2)
Volume		
milliliter (mL)	0.06102	cubic inch (in^3)
Mass		
gram (g)	0.03527	ounce, avoirdupois (oz.)

Mineralogical and Chemical Composition of Saprolite from South Fork Brokenback Run Watershed, Shenandoah National Park, VA

Joy Pochatila¹, Blair F. Jones, Kathryn M. Conko, and Daniel M. Webster

ABSTRACT

This study of mineral assemblages within the weathering profile at South Fork Brokenback Run, Shenandoah National Park, Virginia, extends previous research that focused on mass-balance calculations employing idealized formulation for the dissolution of primary mineral reactants in the granitic bedrock and for resulting mineral products in the overlying saprolite. From two cores of the granite weathering profile (regolith) obtained in an earlier investigation, mineralogical and chemical analyses of five physically separated fractions of the saprolite were obtained for discrete depth increments. X-ray diffraction (XRD) analyses identified quartz, potassium feldspar, biotite, amphibole, plagioclase, illite, kaolinite, and goethite, in addition to a 2:1 expandable clay, considered an aluminous smectite. CLAYFORM, a computer program for calculating structural formulae of clay minerals from elemental chemical analyses, was used to characterize the composition of the finest fractions containing the most smectite, which appeared to range from $K_{0.4}(Si_{3.0}Al_{1.0})_{4.0}(Al_{2.0}Mg_{0.3})_{2.33}O_{10}(OH)_2$ to $Ca_{0.3}(Si_{3.0}Al_{1.0})_{4.0}(Al_{2.0}Mg_{0.2})_{2.33}O_{10}(OH)_2$. This clay was taken to be an important intermediate in the weathering of the granite.

INTRODUCTION

Geochemical research on natural weathering has often been directed toward explanations of the chemical composition of surface water and ground water resulting from subsurface water-rock interactions. These interactions are often defined as the incongruent dissolution of primary minerals, such as feldspar, producing secondary weathering products, such as clay minerals, and solute fluxes, (Meunier and Velde 1979). The composition of the clay-mineral product species is rarely determined. The purpose of this investigation was to identify and chemically characterize the mineralogy of the saprolitic weathering profile at the South Fork Brokenback Run (SFBR) watershed.

The South Fork Brokenback Run watershed is on the northern flank of Old Rag Mountain adjacent to Robertson Mountain in the central part of Shenandoah National Park in Madison County, Virginia (figure 1). The area of the forested watershed is approximately 237 ha, and the vegetative cover consists of a second-growth mixed oak-hickory forest dominated by chestnut oak (*Quercus prinus*) and northern red oak (*Q. Rubra*) (Furman and others, 1998).

The soils in the catchment are characterized as Ultisols and are mapped as part of the Tusquitee and Unison Series, which are texturally described as clay loams (Scanlon, 1999).

The Old Rag Granite and related intrusive rocks that underlay the catchment have weathered to saprolite (Piccoli, 1987). The thickness of the saprolite ranges from 0 m at the Brokenback Run stream to more than 20 m on the hillslopes (O'Brien and others, 1997). The variation in the composition of silicate minerals, as described by Piccoli (1987), and Hackley (1999), prompted interest in the compositional variation in the weathering products.

Recent investigations, such as O'Brien and others, and Furman and others, attempted to determine the contribution of primary mineral weathering reactions to observed stream chemistry at SFBR. The authors in both investigations assumed that stream chemistry was the result of

¹ Topographic Engineering Center, U.S. Army Corps of Engineers, Alexandria, VA

simple reactions between rainwater and the primary mineral phases in the bedrock. O'Brien and others, concluded that their estimated weathering reactions were at times inconsistent with field observations. For example, the precipitation of amorphous silica was predicted to occur in surface waters of the SFBR catchment. Amorphous silica, however, was not observed to form in any of the streams, suggesting a potential sink for silica was excluded, which was probably a clay-mineral product. The mass-balance model results of Furman and others could provide only a rough estimate of the weathering processes because highly idealized mineral compositions were utilized in the calculations. Further, Na-saturated smectite was the principal clay-mineral product chosen for their analysis. However, it is unrealistic for this setting where base-cation selectivity would favor Ca or K occupying exchange sites in the mineral structure (Drever, 1982).

In the present study, which was done in support of improved mineral-solute mass balance modeling, the primary objective was to identify and characterize the mineral assemblage in the saprolitic weathering profile above the granitic bedrock. Two cores representing saprolite up to 25m depth were sampled for mineral assemblages. Methods used to determine these assemblages included physical size fractionation of samples from discrete depth-intervals, followed by X-ray diffraction (XRD) and chemical analyses. The secondary objective was to estimate the specific chemical formulae for 2:1 layer clay minerals identified in the weathering profile. This was accomplished by using the mineralogic and compositional data from XRD and chemical analyses for the three finest fractions of each sample (n=21) to obtain 2:1 clay-mineral formulae with the aid of the computer model CLAYFORM (Bodine, 1987).

METHODS

Saprolite Sampling

Samples of the weathering profile at Old Rag Mountain were obtained from two cores from boreholes drilled at UTM 732687 4271518 (fig. 1). The U.S. Geological Survey installed a well at this location in August 1983 to a depth of 23.8 meters and the cores were obtained as part of that effort (Owen Bricker, USGS, personal communication, 2002). These cores were subsequently referred to as core 2 (OR83-2) and core 3 (OR83-3) even though core from the first borehole was not retained. For consistency, the same nomenclature was adopted here. The cores were stored in boxes, each containing intervals of approximately 3.7 meters. Cores 2 and 3 were 18.6 and 25.4 m in length, respectively, and were generally composed of highly weathered material. Samples illustrating different lithological structures and color in the weathering profile were taken from the cores for analysis in the present study.

Mineral Separation Technique

In addition to X-ray diffraction (XRD) examination of bulk material, specimens of the Old Rag weathering profile were separated into four particle-size ranges to improve the identification of matrix mineral phases and enhance the purity of the finest-grained clays. Whole samples were dispersed in water ultrasonically to prepare slurries from which <1, <0.5, <0.1, and <0.03 μm fractions were obtained by centrifugation. Centrifugation times were set at 3,000 RPM for two minutes; 4,000 RPM for four minutes; 10,000 RPM for ten minutes; and 20,000 RPM for one hour, respectively. The particulates in the resulting supernatant liquids were consolidated into pellets by centrifugation at a full 20,000 RPM long enough to clarify the solutions. The <0.03 μm fractions required ultra-centrifugation at 40,000 RPM for at least one hour to consolidate the solid materials. As the attempt was made to obtain finer grain-sized fractions, the number of core samples yielding sufficient material for chemical analysis decreased.

X-ray Diffraction Procedures

Powders of whole samples were placed on glass mounting substrates with one or two drops of an adhesive solution containing amyl acetate and ethyl cellulose. The mixtures were air-dried quickly, allowing the crystallites to retain random orientation. Size-fractionated clays were mounted to enhance basal reflection orientation by spreading the moist material on glass substrates that were dried slowly at room temperature. The slides were then analyzed following separate operational treatments to obtain basal-peak response: untreated, solvated with ethylene glycol, and heated at 550°C for one hour or longer. All specimens were analyzed with long-fine focused $\text{CuK}\alpha$ radiation, spectrally isolated with a graphite-crystal monochromator. The scan rate was $1^\circ 2\theta$ per minute, using a soller slit of 1° and a receiving slit of 0.1 mm, with an antiscatter slit of 1 mm. All sample slides were scanned from 2 to $66^\circ 2\theta$.

Chemical Analysis

The bulk and sized fractions (depending on amount of sample actually separated) were chemically analyzed for major and minor cation concentrations. The samples were weighed into a teflon vessel and completely digested using a combination of concentrated Fisher Optima double-distilled HNO_3 and hydrofluoric (HF) acids in a laboratory microwave oven (MDS 2100, CEM Corporation). The samples were brought to 50 ml volume with deionized water, yielding an acid concentration in the sample of approximately 20% HNO_3 and 10% HF.

Total concentrations of major cations -- silicon (Si), aluminum (Al), and iron (Fe)-- and the minor cations-- sodium (Na), potassium (K), calcium (Ca), magnesium (Mg), manganese (Mn), strontium (Sr) and titanium (Ti)-- were determined by inductively coupled plasma optical emission spectroscopy (ICP-OES) using a Perkin Elmer P-2 instrument.

Quality assurance and quality control of the laboratory analyses were continuously carried out through a series of approved methods (Pirkey and Glodt, 1998). The quality assurance directly related to instrument analysis included daily calibration and verification of the calibration by running blanks and standard reference materials (SRM) periodically during the analytical run. For each analyte a four- or five-point standard concentration curve (including blank) with an r^2 value of 0.999 or better was constructed. At the beginning and end of each analytical session, the standard calibration was verified by running additional standard solutions and SRM. During the analysis, known standard solutions and SRM were run periodically (every fifth to tenth sample) to verify the precision and accuracy of the analysis, and to monitor instrument drift. Samples with enough mass (> 1.0 g) were analyzed in duplicate or triplicate to give an indication of potential analytical error and to evaluate sample homogeneity. These replicate samples were collected and treated in the same manner as the other samples and the results were arithmetically averaged for mass-balance modeling.

Estimating mineral abundance

After X-ray diffractograms were obtained for all fractions, and identification completed for the major mineral phases, an attempt was made to assess relative quantities. The relative abundance of each mineral identified by XRD was approximated by the intensity of the principal reflections and tabulated by simple numerical order. Where possible in the clay mineral fractions, relative abundance was estimated by both peak height and area underneath the peak. For example, if the 7\AA peak identifying kaolinite was half the area of the expandable $10\text{-}14\text{\AA}$ peak attributed to a 2:1 layer silicate, it was assumed that kaolinite was half as abundant as smectite.

Use of CLAYFORM to develop a clay-mineral formula

Upon the identification of a 2:1 expandable layer silicate through XRD, the computer model CLAYFORM (Bodine, 1987) was used to develop a clay-mineral formula for this material. (It should be noted that the basal spacing of the 2:1 layer silicate was expandable by glycol to 17Å, collapsing to about 10Å at 550 C, and thus classified as smectite). CLAYFORM apportions weight-percent chemical data into a formula based on a general, user-defined stoichiometry (Bodine, 1987). In this study, a 2:1 phyllosilicate mineral structure was specified. The analyzed constituents were distributed into appropriate tetrahedral, octahedral, and interlayer cation sites, as well as anion and hydroxyl sites, and the CLAYFORM output was a structural formula resulting from the specifications assigned to each sample (Bodine, 1987).

Where sufficient material could be separated for major-ion chemical analysis of the clay fractions, the cation concentrations (as weight-percent oxides) in the samples were used as input data for the CLAYFORM computations. However, these values represented the weight percentage of each oxide for the entire mineral assemblage in the sample. Therefore, steps were taken to isolate the constituents associated only with the smectite by subtracting the composition of other minerals from the analysis. The technique was to subtract the ideal stoichiometry of other phases present in the finer fractions ($< 0.5 \mu\text{m}$, $< 0.1 \mu\text{m}$, and $< 0.03 \mu\text{m}$). For example, if all the Na_2O and CaO in the sample could be attributed to plagioclase identified in the bulk fraction, then equivalent weight percent of Na_2O and CaO , as well as corresponding amounts of SiO_2 and Al_2O_3 needed to form the plagioclase were subtracted from the total weight percent of the sample. These steps were repeated for each non-smectite mineral identified. Appropriate amounts of SiO_2 and Al_2O_3 were subtracted from the sample when kaolinite was identified. Similarly, when illite was identified, corresponding amounts of K_2O , MgO , SiO_2 , and Al_2O_3 were subtracted from the sample, and appropriate amounts of Fe_2O_3 were subtracted for the occurrence of goethite. These subtractions were made for all three finer fractions, depending on quantity of the smectite minerals associated with the bulk analysis of the specific sample. CLAYFORM calculated the mole percent of each oxide based on the remaining weight percent and distributed the residual cations to the tetrahedral, octahedral, and interlayer positions appropriate for a smectite formula.

MINERALOGICAL AND CHEMICAL COMPOSITION OF SAPROLITE

Mineralogy

Descriptions of the cores are given in tables 1 and 2. The mineralogy of the Old Rag weathering profile is organized and reported by size fraction and profile depth in tables 3-5. The bulk samples were dominated by quartz and potassium feldspar, with only minor amounts of plagioclase feldspar, mica, and clay minerals (table 3). Muscovite or sericite mica were differentiated by sharpness of the basal reflections. Illite abundance generally decreased with average grain size. In all fractions examined, abundant K-spar commonly obscured the reflections for plagioclase. Smectite was most significant in the finer clay fractions, which otherwise were largely composed of kaolinite and goethite, with very minor amounts of a 10Å phase and amphibole (table 4). Some amorphous material was suspected, but presumably this was included in the fraction analysis and had a minimal effect on the composition of the smectite. In the coarser clay fractions, the smectite was most positively identified in thin horizons at the top and middle of the profile. Similar smectite enrichment was observed in the ultrafine fractions at the middle and bottom of the profile (table 5). With regard to the overall phase assemblage, the XRD results reported in tables 3-5 reveal considerable variability with depth in the profile. There is some tendency for middle horizons (approximately 12m to 15m depth) to reflect a higher percentage of mafic material, such that goethite and amphibole can be associated with more abundant smectite. Also, an inverse relation between kaolinite and illite was observed in finer fractions; that is, where kaolinite was abundant, a 10Å phase was only a minor presence.

Chemical Analysis

The results of chemical analysis, expressed as percent oxide composition, for each size fraction where there was enough material (tables 8-11) indicated that SiO_2 and Al_2O_3 were the dominant constituents, representing 28-68% and 11-40% of each sample, respectively. Fe_2O_3 was the third most abundant oxide, with percentages ranging from 1-28%. The percentages of the base-cation oxides showed similar values; however, Na_2O appeared to be the least abundant. The sums of the oxides do not necessarily equal 100%. This is due to the presence of unanalyzed organic material, water, and minor elements in the samples, as well as slight variability due to sample heterogeneity and inherent analytical error. These data, in conjunction with the XRD results, were used to estimate the chemical formulae for the expandable (smectite) phase.

CLAYFORM Results

As noted earlier, the results of chemical analysis of the $< 0.5 \mu\text{m}$, $< 0.1 \mu\text{m}$, and $< 0.03 \mu\text{m}$ fractions were used as input to the computer model, CLAYFORM (Bodine, 1987). A summary of the results of the calculated 2:1 expandable phase (smectite) formula is given in tables 10-12. The tables present the distribution of the major cations in the tetrahedral, octahedral, and inter-layer positions, as well as the respective layer charges (the positively charged octahedral layer and interlayer balance the negatively charged tetrahedral layer).

Certain assumptions in the results from CLAYFORM need to be pointed out. Goethite was the only pure, iron-bearing mineral phase identified in the XRD analyses, and it was ubiquitous in the ultrafine fractions (< 0.1 and $< 0.03 \mu\text{m}$). The assumption was then made that all of the Fe_2O_3 in the samples could be attributed to goethite and, therefore, Fe_2O_3 could be eliminated from calculation of the smectite formula. As to be expected for a smectite, Si^{4+} and Al^{3+} cations were assigned to tetrahedral positions, whereas the small amount of Mg^{2+} , plus the Al^{3+} in excess of tetrahedral occupancy, was retained in the octahedral sites. With the formulae presented for the $< 0.5 \mu\text{m}$ fraction, only K^+ is shown as occupying the interlayer position, because of the negligible concentration of Ca (Table 12). However, in the < 0.1 and $< 0.03 \mu\text{m}$ fractions (Tables 13 and 14, respectively) the interlayer position was assigned to both K^+ and Ca^{2+} (the only suitable sites for ions of this size).

Despite the large variation in the formulae derived for all the clay fractions, each fraction shared some fundamental characteristics. First, all the formulae that were charge-balanced with reasonable assignment of constituent sites had a Si/Al ratio close to 1.0. This was particularly evident in the formulae associated with the $< 0.5 \mu\text{m}$ fraction (Table 12). The accommodation of minor Mg in the octahedra (balanced in part by interlayer cations) was what produced formulae for Al-smectite (beidellite) rather than kaolinite. Where there was a deficiency in either of the tetrahedral cations, a charge-balanced formula could not be obtained. This problem can be readily recognized if the sum of interlayer cations ($\text{K} + \text{Ca}$) exceeds 1.0 (tables 11 & 12). To bracket the variation in the composition for mineral-solute mass-balance calculations, idealized formula end-members that reflected the characteristics above were developed from the whole suite of CLAYFORM results. The end-members chosen to represent the compositional range for 2:1 layer silicate were K- and Ca-saturated beidellitic smectite. The formulae for this smectite ranged from $\text{K}_{0.4}\text{Si}_{3.0}\text{Al}_{3.0}\text{Mg}_{0.3}\text{O}_{10}(\text{OH})_2$ to $\text{Ca}_{0.3}\text{Si}_{3.0}\text{Al}_{3.0}\text{Mg}_{0.2}\text{O}_{10}(\text{OH})_2$, respectively.

SUMMARY

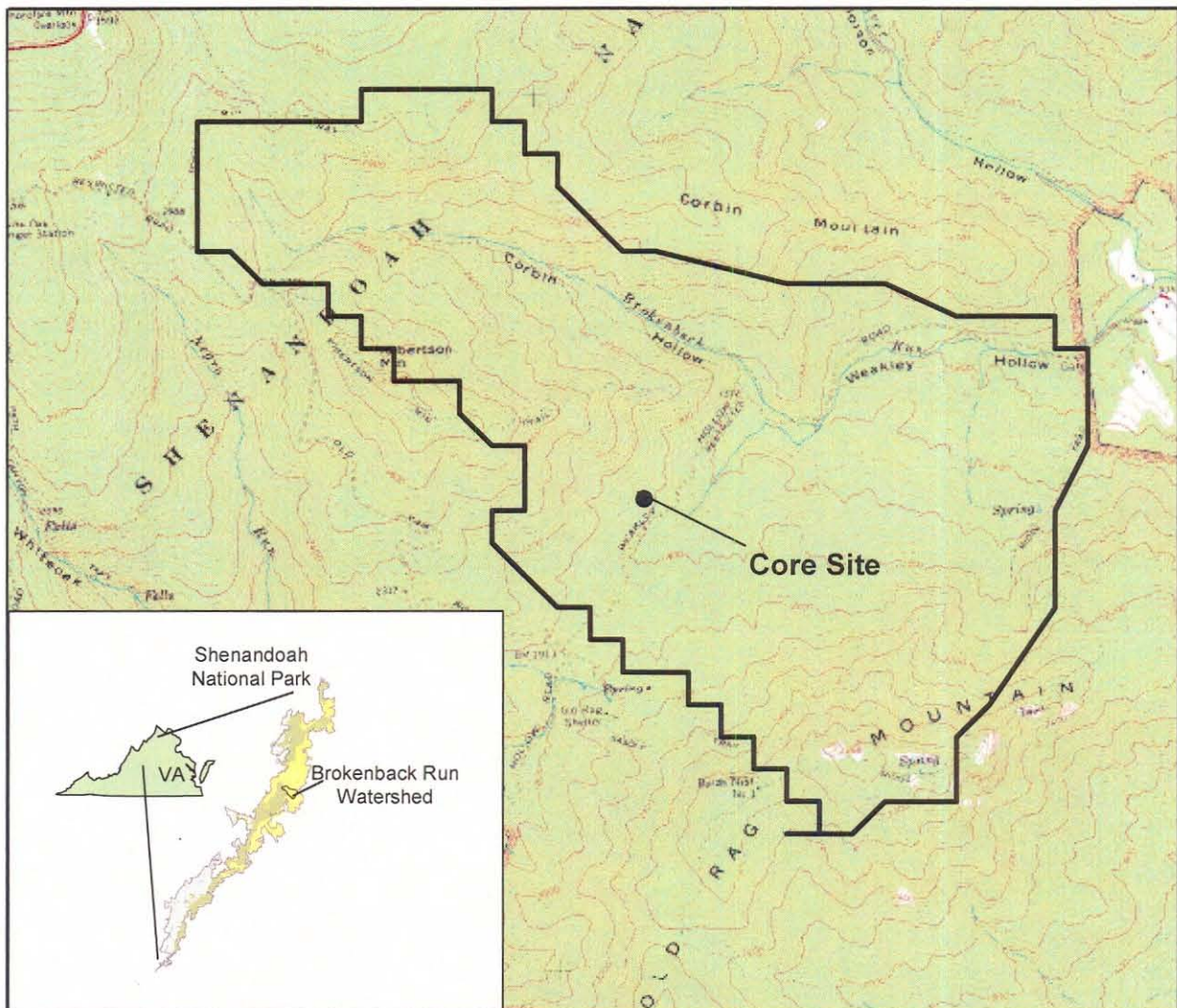
Rigorous assessments of solute mass fluxes from watersheds can be achieved when reactants and products in mineral-weathering reactions are fully characterized. The inclusion of the chemical and mineralogical compositions of bedrock and saprolite in mass-balance calculations improves the quantification of balanced weathering reactions. The purpose of this study was to identify and chemically characterize the mineralogy of the saprolitic-weathering profile at SFBR. XRD analysis of the bulk and fine clay-size fractions ("bulk" or greater than 1 μm , less than 1 μm , less than 0.5 μm , less than 0.1 μm , and less than 0.03 μm) of two drill core samples was employed to determine the relative abundance of mineral phases at varying depths within the weathering profile. Quartz and feldspar were the principal phases identified in the bulk samples, whereas the fine fractions were characterized by an assemblage consisting of kaolinite, an expandable 2:1 clay, a 10Å phase (illite or mica), goethite, and traces of amphibole, all in highly variable amounts. Chemical analyses of the samples were performed to determine the major and minor cation concentrations of the material. The program CLAYFORM (Bodine, 1987) was used in conjunction with the chemical and XRD data to estimate the formula for the expandable 2:1 clay mineral phase. This phase was determined to be a K- or Ca-saturated beidellitic smectite very close to kaolinite in composition, with a formulae ranging from $\text{K}_{0.4}\text{Si}_{3.0}\text{Al}_{3.0}\text{Mg}_{0.3}\text{O}_{10}(\text{OH})_2$ to $\text{Ca}_{0.3}\text{Si}_{3.0}\text{Al}_{3.0}\text{Mg}_{0.2}\text{O}_{10}(\text{OH})_2$, respectively. The identification and analysis of these secondary minerals is expected to increase understanding of the incongruent dissolution reactions and concomitant solute fluxes that occur in headwater streams as a result of bedrock weathering.

ACKNOWLEDGMENTS

The authors thank Owen Bricker (USGS) for permitting us to sample the drill core obtained from SFBR, and for discussion and comments on the manuscript. Early motivation for this research was provided by discussions with Jeffrey Raffensperger (currently USGS, previously University of Virginia). We also thank Janet Herman (University of Virginia) for providing editing and review comments during the writing process. Support for Joy Pochatila was provided in part by the University of Virginia.

REFERENCES

- Bodine, M.W., 1987, CLAYFORM; a Fortran 77 computer program apportioning the constituents in the chemical analysis of a clay or other silicate mineral into a structural formula: *Computers & Geosciences*, 13 (1) 77-88.
- Drever, J.I., 1997, *The Geochemistry of Natural Waters*: Prentice-Hall, Englewood Cliffs, N.J., 436 pp.
- Furman, T., Thompson, P., Hatchl, B., 1998, Primary mineral weathering in the Central Appalachians; a mass balance approach: *Geochimica et Cosmochimica Acta*, 62 (17) 2889-2904.
- Hackley, Paul C., 1999, Petrology, geochemistry, and field relations of the Old Rag Granite and associated charnockitic rocks, Old Rag Mountain 7.5' quadrangle, Madison and Rappahannock Counties, Virginia: MS thesis, George Washington University, Washington, DC, 244p.
- Meunier, A., Velde, B., 1979, Weathering mineral facies in altered granites: the importance of local small-scale equilibria: *Mineralogical Magazine* (43) 261-268.
- O'Brien, A.K., Rice, K.C., Bricker, O.P., Kennedy, M.M., Anderson, R.T., 1997, Use of geochemical mass balance modeling to evaluate the role of weathering in determining stream chemistry in five Mid-Atlantic watersheds on different lithologies: *Hydrological Processes*, 11 (7) 719-744.
- Piccoli, P., 1987, Petrology and geochemistry of the Old Rag Granite on Old Rag Mountain: MS Thesis. University of Pittsburgh, Pittsburgh, PA, United States
- Pochatila, J., 2000, Geochemical Investigation of Weathering Processes in a Forested-Headwater Catchment: A Mass-Balance Approach, MS Thesis. University of Virginia.
- Pirkey, K., Glodt, S., 1998, Participation in performance-evaluation studies by the U.S. Geological Survey National Water Quality Laboratory: U.S. Geological Survey Report: FS 0023-98. 6 pp.
- Scanlon, T., 1999, Modeling stream discharge and dissolved silica variations in a forested-headwater catchment: a hydrological pathways approach: MS Thesis. University of Virginia, Charlottesville, VA, United States.



SCALE 1:25,000

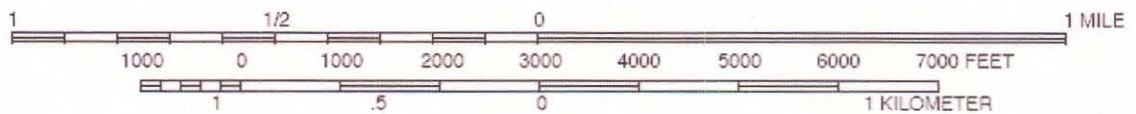


Figure 1: Site map of Brokenback Run Watershed, Shenandoah National Park, Madison County, VA. The core site is located at latitude 38° 33' 08" N, longitude 078° 19' 46" W. (Topographic base map is portion of US Geological Survey 1:25,000 "Old Rag Mountain" Quadrangle. The Shenandoah Watershed Study (SWAS) at the University of Virginia is credited with images of the outline of Shenandoah National Park and Brokenback Run watershed.)

Table 1: Description of Saprolite Weathering Profile at Old Rag Mountain (Core 2, 83-2)

Depth in meters	Grain Size	Color	Observed Changes on drying
0-0.16m	sand – silt	light brown	light brown, sandy-silt soil
0.61-8.2	silt	yellowish orange	yellowish orange, silt
8.2-13.1	clayey – silt	white	very white, chalky layer with clay/silt texture
13.1-17.4	silt	yellowish orange	yellowish orange, silt
17.4-18.6	clay	light orange	Light orange/golden clay texture

Table 2: Description of Saprolite Weathering Profile at Old Rag Mountain (Core 3, 83-3)

Depth in meters	Grain Size	Color	Observed Changes on drying
0-2.4m	sand-silt	light brown to yellowish orange (golden)	texture change from light brown soil to golden sand
2.4-8.2	silt	yellowish white	yellowish white silty texture
8.2-14.0	clay	yellowish orange	yellowish orange clay texture; stratified from 8.2 –8.9m
14.0-16.8	clay	white	white, clayey texture
16.8-18.0	clay	yellowish orange	yellowish orange clay texture
18.3	clay	white	white, clayey texture
18.3-22.0	clay	yellowish orange	yellowish orange clay texture
19.8-23.5	clay	white	white, clayey texture
23.5-25.4	clay	yellowish orange	yellowish orange clay texture

Table 3: XRD results for whole-rock (bulk) mineralogy of samples from the Old Rag Granite weathering profile. The relative abundance is indicated by the integers based on the principal-peak intensity for the mineral identified. Lower integers indicate higher intensity and abundance. A zero indicates no conclusive identification.

Core #	Depth (m)	Quartz	K-spar	Mica	Amphibole	Plagioclase	Total Clay
2	0.6	1	2	0	0	0	3
3	0.6	1	2	4	0	0	3
2	2.4	1	2	4	0	0	3
3	2.4	1	2	4	0	0	3
2	6.1	1	2	4	0	0	3
3	6.4	1	2	4	0	0	3
2	8.2	2	1	0	0	4	3
3	9.1	1	0	0	0	0	4
2	13.4	1	3	5	0	4	2
2	15.5	1	2	0	4	0	3
2	17.4	1	2	4	0	0	3
2	18.6	1	0	4	0	3	2
3	19.8	1	3	4	0	0	2
3	20.4	1	2	0	0	3	4
3	23.4	1	0	0	0	2	3

Table 4a. XRD results for clay mineralogy (< 1.0 μm) from the Old Rag Granite weathering profile. Illite refers to a broadened 10Å reflection and can include weathered biotite. The relative abundance is indicated by the integers based on the principal-peak intensity for the mineral identified. Lower integers indicate higher intensity and abundance. A zero indicates no conclusive identification.

Core #	Depth (m)	Kaolinite	Smectite	Illite	Amphibole	Goethite
2	0.6	1	0	2	0	4
3	0.6	1	3	2	0	4
2	2.4	1	2	3	5	4
3	2.4	2	3	1	0	4
2	6.1	1	0	2	0	0
3	6.4	1	0	2	3	4
2	8.2	1	0	2	0	0
3	9.1	1	3	2	4	5
2	13.4	2	0	1	0	0
2	15.5	2	0	1	0	0
2	17.4	2	0	1	0	0
2	18.6	2	0	1	0	0
3	19.8	1	3	2	5	4
3	20.1	2	0	1	0	0
3	23.4	2	3	1	5	4

Table 4b. XRD results for clay mineralogy (< 0.5 μm) from the Old Rag Granite weathering profile. A question mark indicates possible identification in a trace amount. Refer to caption for table 4a for further information.

Core #	Depth (m)	Kaolinite	Smectite	Illite	Amphibole	Goethite
3	0.4	1	4	3	0	2
2	2.7	1	3	4	?	2
2	5.2	1	2	4	?	2
3	6.7	1	4	2	0	3
2	8.5	1	3	4	0	2
3	9.4	1	4	5	3	2
3	12.8	1	2	3	5	4
3	12.9	2	3	5	4	1
2	14.0	1	4	2	5	3
3	15.2	1	4	2	0	3
2	18.0	1	3	4	?	2
3	20.1	1	4	2	0	3
3	23.2	1	4	3	?	2

Table 5a: XRD results for ultrafine (< 0.1 μm) clay mineralogy from the Old Rag Granite weathering profile. Illite refers to a broadened 10 \AA reflection and can include weathered biotite. The relative abundance is indicated by the integers based on the principal-peak intensity for the mineral identified. Lower integers indicate higher intensity and abundance. A zero indicates no conclusive identification.

Core #	Depth (m)	Kaolinite	Smectite	Illite	Amphibole	Goethite
3	0.6	1	3	4	5	2
2	2.4	1	3	5	4	2
2	13.4	2	1	5	4	3
3	19.8	1	3	5	4	2
3	20.4	1	3	5	4	2
3	23.4	3	1	5	4	2

Table 5b: XRD results for ultrafine (<0.03 μm) clay mineralogy from the Old Rag Granite weathering profile. A question mark indicates possible identification in a trace amount. Refer to caption for table 5a for further information.

Core #	Depth (m)	Kaolinite	Smectite	Illite	Amphibole	Goethite
3	0.4	1	4	3	0	2
2	2.4	1	3	4	5	2
2	2.7	1	3	4	5	2
2	5.2	1	2	4	0	3
3	6.7	1	3	4	?	2
2	8.6	1	2	4	?	3
3	9.5	2	3	4	5	1
3	12.8	2	3	4	5	1
3	12.9	2	1	5	3	4
2	14.0	2	3	5	4	1
3	15.2	2	1	?	?	3
2	18.0	1	4	3	?	2
3	19.8	2	1	0	4	3
3	20.4	1	3	5	4	2
3	23.2	1	3	2	4	4
3	23.4	2	3	5	4	1

Table 6: Chemical composition of whole rock (bulk sample, >1 μm) specimens from the Old Rag Granite weathering profile. Element concentrations are expressed in weight percent oxide.

Core #	Depth (m)	SiO ₂	Al ₂ O ₃	Fe ₂ O ₃	K ₂ O	CaO	MgO	Na ₂ O	MnO	TiO ₂	SrO
3	0.4	46	30	7.6	1.7	0.07	0.42	0.37	0.02	0.6	<0.01
2	0.6	45	40	5.6	0.5	0.24	0.54	0.02	0.02	0.3	0.01
2	2.4	32	24	7.5	1.3	0.44	0.68	0.08	0.03	0.6	0.01
3	2.7	68	19	3.7	2.8	0.06	0.46	0.56	0.03	0.5	0.01
2	5.2	54	34	5.2	3.1	0.16	0.32	0.15	0.02	0.3	0.01
3	6.7	52	29	4.9	4.0	0.26	1.16	0.09	0.03	0.6	0.01
2	8.5	57	33	2.5	3.8	0.18	0.26	0.26	0.01	0.2	0.01
3	9.4	48	21	14.2	1.0	0.19	1.95	0.13	0.16	4.3	<0.01
2	11.0	56	34	2.4	4.5	0.39	0.50	0.44	0.03	0.3	0.01
2	12.8	53	17	10.3	0.7	0.51	0.79	0.15	0.20	0.6	0.01
3	13.7	33	19	16.5	0.5	0.38	1.40	0.05	0.47	1.6	<0.01
2	14.0	53	14	5.1	5.3	0.29	0.73	0.26	0.08	0.5	0.01
2	15.4	61	16	17.9	0.8	0.50	1.17	0.14	0.08	1.0	0.02
3	20.1	52	30	1.1	3.5	0.05	0.26	0.32	0.01	0.2	<0.01
3	23.2	45	30	6.2	1.0	0.12	0.77	0.76	0.07	0.7	<0.01

Table 7: Chemical composition of the < 0.5 μm fraction of samples from the Old Rag Granite weathering profile. Element concentrations are expressed in weight percent oxide.

Core #	Depth (m)	SiO ₂	Al ₂ O ₃	Fe ₂ O ₃	K ₂ O	CaO	MgO	Na ₂ O	MnO	TiO ₂	SrO
2	2.4	48	20	3.3	0.18	0.01	0.03	0.24	0.01	0.24	<0.01
3	2.7	54	20	16	1.10	0.02	0.20	0.35	0.04	0.07	<0.01
2	5.2	50	26	9.1	0.37	0	0.09	0.23	0.01	0.87	<0.01
3	6.7	54	27	11	1.20	0.02	0.20	0.19	0.01	0.73	<0.01
2	8.5	57	24	2.6	0.68	0.01	0.03	0.34	0.02	0.33	<0.01
3	9.4	35	13	23	0.19	0.08	0.30	0.28	0.22	3.20	<0.01
3	12.2	47	11	38	0.25	0.10	0.10	0.30	0.28	0.27	<0.01
2	12.8	50	28	12	0.31	0.03	0.10	0.22	0	0.15	<0.01
2	14.0	46	20	27	0.27	0.20	0.20	0.19	0.31	0.72	<0.01
3	15.2	51	19	6.6	2.40	0.01	0.05	0.31	0.04	0.92	<0.01
2	18.0	40	21	30	0.33	0.20	0.30	0.24	0.17	0.65	<0.01
3	20.1	56	17	11	1.50	0.04	0.20	0.24	0.12	0.67	<0.01
3	23.2	68	28	1.4	1.10	0.01	0.06	1.00	0.01	0.17	<0.01

Table 8: Chemical composition of the < 0.1 μm fraction of samples of the Old Rag Granite weathering profile. Values are expressed as percent oxide compositions.

Core	Depth (m)	SiO ₂	Al ₂ O ₃	Fe ₂ O ₃	K ₂ O	CaO	MgO	Na ₂ O	MnO	TiO ₂	SrO
2	2.4	29.1	33.8	14.3	0.45	0.39	0.81	0.20	0.03	0.47	0.01
3	2.7	33.1	28.0	16.4	0.82	0.43	1.29	0.10	0.02	0.52	0.02
2	12.8	40.2	23.8	15.6	0.41	1.01	0.41	0.05	0.10	0.67	0.04
3	15.2	31.0	22.7	17.6	0.22	0.39	0.98	0	0.09	3.17	<0.01
3	20.1	37.0	23.8	9.7	0.72	0.39	0.68	0.94	0.15	1.83	0.02
3	23.2	32.4	25.5	15.2	0.23	0.59	1.23	1.55	0.38	0.67	<0.01

Table 9: Chemical composition of the < 0.03 μm fraction of samples of the Old Rag Granite weathering profile. Values are expressed as percent oxide compositions.

Core #	Depth (m)	SiO ₂	Al ₂ O ₃	Fe ₂ O ₃	K ₂ O	CaO	MgO	Na ₂ O	MnO	TiO ₂	SrO
2	2.4	28.0	29.7	19.2	0.54	0.62	0.32	0.04	0.04	0.68	0.01
3	15.2	31.2	19.7	23.4	0.39	0.69	1.19	0	0.12	3.84	0.01
3	20.1	36.2	24.9	17.0	0.87	0.67	1.59	2.83	0.22	2.50	0.03
3	23.2	40.6	29.1	28.0	0.40	0.95	0.99	2.43	0.72	1.50	0.01

Table 10: Mineral formulae for aluminous smectite (beidellite) calculated by CLAYFORM using chemical analyses of < 0.5 μm fraction of samples from the Old Rag Granite weathering profile. Layer charges are given in parentheses below the cations present in each layer.

Depth (m)	Interlayer charge	Tetrahedral layer (charge)	Octahedral layer (charge)	Mineral Formula
0.6	K (0.09)	Si, Al (-0.98)	Al, Mg (0.89)	$\text{K}_{0.09}\text{Si}_{3.02}\text{Al}_{3.09}\text{Mg}_{0.29}\text{O}_{10}(\text{OH})_2$
2.4	K (0.07)	Si, Al (-0.77)	Al, Mg (0.70)	$\text{K}_{0.07}\text{Si}_{3.22}\text{Al}_{2.97}\text{Mg}_{0.05}\text{O}_{10}(\text{OH})_2$
2.4	K (0.34)	Si, Al (-1.02)	Al, Mg (0.68)	$\text{K}_{0.33}\text{Si}_{2.98}\text{Al}_{3.06}\text{Mg}_{0.28}\text{O}_{10}(\text{OH})_2$
6.7	K (0.08)	Si, Al (-0.94)	Al, Mg (0.86)	$\text{K}_{0.08}\text{Si}_{3.06}\text{Al}_{2.96}\text{Mg}_{0.13}\text{O}_{10}(\text{OH})_2$
8.5	K (0.18)	Si, Al (-0.93)	Al, Mg (0.75)	$\text{K}_{0.18}\text{Si}_{3.07}\text{Al}_{3.15}\text{Mg}_{0.05}\text{O}_{10}(\text{OH})_2$
9.4	K (0.27)	Si, Al (-1.00)	Al, Mg (0.73)	$\text{K}_{0.27}\text{Si}_{3.00}\text{Al}_{3.07}\text{Mg}_{0.26}\text{O}_{10}(\text{OH})_2$
12.2	K (0.06)	Si, Al (-0.93)	Al, Mg (0.87)	$\text{K}_{0.06}\text{Si}_{3.07}\text{Al}_{3.14}\text{Mg}_{0.12}\text{O}_{10}(\text{OH})_2$
13.7	K (0.08)	Si, Al (-1.03)	Al, Mg (0.95)	$\text{K}_{0.08}\text{Si}_{2.97}\text{Al}_{3.04}\text{Mg}_{0.46}\text{O}_{10}(\text{OH})_2$
14.0	K (0.09)	Si, Al (-0.99)	Al, Mg (0.90)	$\text{K}_{0.09}\text{Si}_{3.01}\text{Al}_{3.08}\text{Mg}_{0.32}\text{O}_{10}(\text{OH})_2$
15.2	K (0.13)	Si, Al (-1.00)	Al, Mg (0.86)	$\text{K}_{0.13}\text{Si}_{3.00}\text{Al}_{3.16}\text{Mg}_{0.26}\text{O}_{10}(\text{OH})_2$
20.1	K (0.45)	Si, Al (-1.07)	Al, Mg (0.62)	$\text{K}_{0.45}\text{Si}_{2.93}\text{Al}_{2.99}\text{Mg}_{0.42}\text{O}_{10}(\text{OH})_2$
23.2	K (0.28)	Si, Al (-0.96)	Al, Mg (0.68)	$\text{K}_{0.28}\text{Si}_{3.04}\text{Al}_{3.12}\text{Mg}_{0.10}\text{O}_{10}(\text{OH})_2$

Table 11: Mineral formulae for aluminous smectite (beidellite) calculated by CLAYFORM using chemical analyses of <0.1 μm fraction of samples from the Old Rag Granite weathering profile. Layer charges are given in parentheses below the cations present in each layer.

Depth (m)	Interlayer (charge)	Tetrahedral layer (charge)	Octahedral layer (charge)	Mineral Formula
2.4	Ca, K (0.26)	Si, Al (-1.38)	Al, Mg (1.12)	$\text{Ca}_{0.08}\text{K}_{0.10}\text{Si}_{2.63}\text{Al}_{3.61}\text{Mg}_{0.22}\text{O}_{10}(\text{OH})_2^*$
12.8	Ca, K (0.47)	Si, Al (-0.50)	Al, Mg (0.03)	$\text{Ca}_{0.19}\text{K}_{0.09}\text{Si}_{3.5}\text{Al}_{2.44}\text{Mg}_{0.11}\text{O}_{10}(\text{OH})_2^*$
20.1	Ca, K (0.28)	Si, Al (-1.04)	Al, Mg (0.76)	$\text{Ca}_{0.07}\text{K}_{0.15}\text{Si}_{2.96}\text{Al}_{3.19}\text{Mg}_{0.16}\text{O}_{10}(\text{OH})_2$
20.1	Ca, K (0.34)	Si, Al (-0.60)	Al, Mg (0.26)	$\text{Ca}_{0.10}\text{K}_{0.13}\text{Si}_{3.40}\text{Al}_{2.59}\text{Mg}_{0.15}\text{O}_{10}(\text{OH})_2^*$
23.2	Ca, K (0.37)	Si, Al (-0.89)	Al, Mg (0.53)	$\text{Ca}_{0.16}\text{K}_{0.05}\text{Si}_{3.11}\text{Al}_{2.88}\text{Mg}_{0.28}\text{O}_{10}(\text{OH})_2$

*not charge-balanced; therefore, unlikely clay formula

Table 12: Mineral formulae for aluminous smectite (beidellite) calculated by CLAYFORM using chemical analyses of <0.03 μm fraction of samples from the Old Rag granite weathering profiles. Layer charges are given in parentheses below the cations present in each layer.

Depth (m)	Interlayer (charge)	Tetrahedral layer (charge)	Octahedral layer (charge)	Mineral Formula
2.4	Ca, K (0.46)	Si, Al (-0.99)	Al, Mg (0.53)	$\text{Ca}_{0.18}\text{K}_{0.10}\text{Si}_{3.01}\text{Al}_{3.07}\text{Mg}_{0.14}\text{O}_{10}(\text{OH})_2$
15.2	Ca, K (0.72)	Si, Al (-1.21)	Al, Mg (0.49)	$\text{Ca}_{0.32}\text{K}_{0.09}\text{Si}_{2.79}\text{Al}_{2.86}\text{Mg}_{0.55}\text{O}_{10}(\text{OH})_2$
20.1	K (0.17)	Si, Al (-1.11)	Al, Mg (0.95)	$\text{K}_{0.17}\text{Si}_{2.89}\text{Al}_{2.95}\text{Mg}_{0.71}\text{O}_{10}(\text{OH})_2$
23.2	Ca, K (1.34)	Si, Al (-1.36)	Al, Mg (0.02)	$\text{Ca}_{0.10}\text{K}_{1.14}\text{Si}_{2.64}\text{Al}_{2.70}\text{Mg}_{0.99}\text{O}_{10}(\text{OH})_2^*$

*not charge-balanced; therefore, unlikely clay formula